



Optics Letters

Comparison of optical feedback dynamics of InAs/GaAs quantum-dot lasers emitting solely on ground or excited states

LYU-CHIH LIN,¹ CHIH-YING CHEN,¹ HEMING HUANG,² DEJAN ARSENIJEVIĆ,³ DIETER BIMBERG,^{3,4} FRÉDÉRIC GRILLOT,^{2,5} AND FAN-YI LIN^{1,*}

¹Institute of Photonics Technologies, Department of Electrical Engineering, National Tsing Hua University, Hsinchu 300, Taiwan

²LTCI, Télécom ParisTech, Université Paris-Saclay, 46 rue Barrault, 75013 Paris, France

³Institut für Festkörperphysik, Technische Universität Berlin, Berlin 10623, Germany

⁴King Abdulaziz University, Jeddah 21589, Saudi Arabia

⁵Center for High Technology Materials, University of New Mexico, 1313 Goddard SE, Albuquerque, New Mexico 87106, USA

*Corresponding author: fylin@ee.nthu.edu.tw

Received 9 November 2017; revised 5 December 2017; accepted 5 December 2017; posted 6 December 2017 (Doc. ID 312950); published 4 January 2018

We experimentally compare the dynamics of InAs/GaAs quantum dot lasers under optical feedback emitting exclusively on ground states (GSs) or excited states (ESs). By varying the feedback parameters and putting focus either on their short or long cavity regions, various P and chaotic oscillatory states are found. The GS laser is shown to be more resistant to feedback, benefiting from its strong relaxation oscillation damping. In contrast, the ES laser can easily be driven into complex dynamics. While the GS laser is of importance for the development of isolator-free transmitters, the ES laser is essential for applications taking advantages of chaos. © 2018 Optical Society of America

OCIS codes: (140.5960) Semiconductor lasers; (050.2230) Fabry-Perot; (160.4236) Nanomaterials; (190.0190) Nonlinear optics.

<https://doi.org/10.1364/OL.43.000210>

Nonlinear dynamics of quantum-well (QW) semiconductor lasers subject to optical feedback has been studied extensively. By controlling the feedback parameters, various dynamical states such as P , quasi-periodic, and chaotic oscillation states and their routes to chaos (C) have been investigated [1,2]. Self-pulsating dynamics, including RPP, chaotic-like pulsations, and low-frequency fluctuating states in transition from short cavity regions (SCRs) to long cavity regions (LCR) has been analyzed and reported [3–7].

Compared to QW lasers, quantum-dot (QD) lasers have many advantages such as small linewidth enhancement factor [8,9], temperature insensitivity [10], low transparency current [11], and low relative intensity noise [12] benefiting from the three-dimensional carrier confinement [13]. Although the modulation capabilities of QD lasers operating on the ground state (GS) are limited to a few gigahertz at room temperature, except for advanced tunneling structures, large signal operation

at 20 Gbit/s was reported [14,15]. Not surprisingly, QD lasers operating on the excited state (ES) show higher differential gain, smaller nonlinear gain compression [13,16], and broader modulation bandwidths with smaller K -factors [17]. Modulation capabilities up to 25 Gbps on-off keying and 35 Gbps pulse-amplitude modulation for high-speed transmitters have been successfully demonstrated for a 1.3 μm InAs/GaAs QD laser emitting on the ES [13,14,16]. Moreover, near-zero linewidth enhancement factors in ES lasers for chirp-free transmitters have been reported [18].

To understand the nonlinear dynamics of QD lasers under the influence of optical feedback, the feedback sensitivity of QD lasers has been investigated [19,20]. The strong damping of relaxation oscillations in GS lasers is thought to be responsible for insensitivity to optical feedback, which has been demonstrated. Anti-phase dynamics in the GS and ES with $\pi/2$ phase shift has been reported [21]. Switching behavior corresponding to the variation of the modal gain when changing the feedback has been discussed [22]. For QD mode-locked lasers, significant stability deterioration at a certain critical level of optical feedback has been demonstrated [23], as well as a regime of extreme stability [24].

While feedback dynamics of QD lasers emitting on different lasing states has been discussed, most investigations were focused on the LCR [25]. To extend and complete the exploration of the feedback dynamics of QD lasers in the SCR, we study and compare here the dynamics of QD lasers in both the SCR and the LCR. For lasers emitting exclusively on the GS or ES, the feedback characteristics of each emission can be investigated independently. By varying the feedback strength and the external cavity length, various states such as periodic (P), regular pulse package (RPP), frequency-locking (FL), quasi-regular pulsing (QRP), quasi-chaos pulse package (QCPP), and C states are found. The GS laser is shown to be more resistant to the perturbation by feedback, benefiting from its large

damping rate. In contrast, the ES laser can easily be driven into complex dynamics, including the C states.

Figure 1 shows the schematic setup of the QD laser subject to optical feedback. The dynamical characteristics of two Fabry–Perot multimode QD lasers, one emitting exclusively on the GS and one on the ES, are investigated and compared under different operation and feedback conditions. The active regions of both lasers are composed of 10 InAs dot sheets grown in InGaAs QWs by molecular beam epitaxy (MBE) with a dot-in-well structure [26]. The dot densities are around $3 \sim 5 \times 10^{10} \text{ cm}^{-2}$ per layer, and their lateral extensions approach 30 nm. Both laser types have internal cavities of 1 mm long and 2 μm waveguides etched through the active area. The output of the laser towards the left is fed back to the laser cavity through a partially reflecting mirror to form an external cavity with length L_{ext} adjustable from 2 to 50 cm. The boundary separating the SCR and the LCR is defined by the ratio between the frequency of the external cavity f_{ext} and the relaxation oscillation frequency f_{RO} , where $f_{\text{ext}}/f_{\text{RO}} > 1$ belongs to the SCR and $f_{\text{ext}}/f_{\text{RO}} < 1$ is the LCR. A variable optical attenuator is used to adjust the feedback strength ξ_f defined as the ratio of the feedback field to the laser output field. The optical signals are analyzed by an optical spectrum analyzer (Advantest Q8384, 10 pm resolution), and the optical power is measured by a power meter. The electrical signals are detected by two identical high-speed photodetectors (Newport 1544-A, 12 GHz bandwidth) and analyzed by an electrical spectrum analyzer (R&S FSV30, 30 GHz bandwidth) and a real-time oscilloscope (Tektronix TDS 6604, 6 GHz bandwidth, 20 GS/s).

Figures 2(a) and 2(b) show the optical spectra of the GS and ES lasers on a semi-logarithmic scale in free-running conditions. For better comparison, both lasers are biased at 1.5 times their threshold currents ($I_{\text{th}} = 16 \text{ mA}$ for the GS and $I_{\text{th}} = 93 \text{ mA}$ for the ES lasers). The center wavelengths of the GS and ES lasers are 1301.5 and 1227.0 nm, and their f_{RO} are 2.1 and 1.3 GHz, respectively. The corresponding boundaries of the SCR and the LCR for the GS and ES lasers are at L_{ext} of 7.3 and 11.5 cm, respectively. As can be seen from the spectra, the GS laser emits exclusively on the GS without the presence of the ES, and the ES laser emits exclusively on the ES without the presence of the GS. By applying feedback to these lasers, the dynamical states associated with each emission line are individually investigated.

Figure 3 shows the time series and the corresponding power spectra of the dynamical states from the GS laser in the SCR and the LCR. In the SCR at $L_{\text{ext}} = 30 \text{ mm}$, an RPP state is demonstrated in Figs. 3(a) and 3(b) for $\xi_f = 0.826$. Different from the RPP state described in [3] for QW lasers showing a fast oscillation frequency f_{FO} coinciding with f_{ext} , the RPP state observed has f_{FO} around $f_{\text{RO}} = 3 \text{ GHz}$ instead.

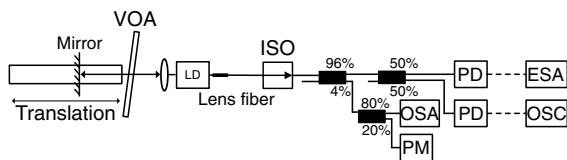


Fig. 1. Experimental setup of a QD laser subject to optical feedback. LD, QD laser; ISO, isolator; PD, high-speed photodetector; ESA, electrical spectrum analyzer; OSA, optical spectrum analyzer; OSC, oscilloscope; PM, power meter.

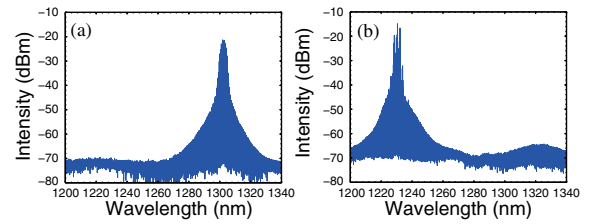


Fig. 2. Optical spectra of the (a) GS and (b) ES lasers at $1.5 \times I_{\text{th}}$ under free-running conditions.

Moreover, the slow oscillation has a frequency $f_{\text{SO}} = 72 \text{ MHz}$ that is much lower than both f_{ext} and f_{RO} . Compared to the RPP states reported in [3] with less than 10 oscillations in each package, more than 40 oscillations are packed in the RPP states found in this GS laser. When ξ_f decreases to 0.731, the laser becomes more stable, and a P state oscillating at f_{RO} , as shown in Figs. 3(c) and 3(d), is found. In the LCR at $L_{\text{ext}} = 100 \text{ mm}$, an FL state [27] is obtained for $\xi_f = 0.634$. As shown in Figs. 3(e) and 3(f), f_{SO} locks to f_{RO} with a rotation number of 1:2. When L_{ext} increases to 200 mm, an FL state with a rotation number of 1:4 is also found. Note that f_{RO} here is increased to about 3 GHz from its free-running value due to the change of the threshold by the feedback [28]. The GS laser subject to feedback is relatively stable such that no C state can be found, even with the strongest feedback attainable in this setup.

Figure 4 shows the time series and corresponding power spectra of the dynamical states from the ES laser in the SCR and the LCR. In the SCR, at $L_{\text{ext}} = 20 \text{ mm}$ and with a strong feedback of $\xi_f = 0.703$, a C state with irregular intensity modulation and a spectrum broadly elevated from the noise floor is shown in Figs. 4(a) and 4(b). When ξ_f decreases to 0.686, a QCPP state is found and shown in Figs. 4(c) and 4(d). Different from an RPP state that has a fast oscillation at f_{ext} [3],

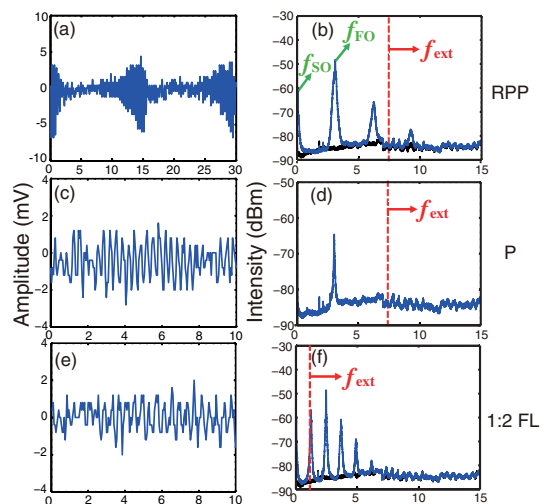


Fig. 3. Time series and corresponding power spectra of the dynamical states obtained experimentally from the GS laser in the SCR and the LCR with $(\xi_f, L_{\text{ext}}) =$ (a, b) (0.826, 30 mm), (c, d) (0.731, 30 mm), and (e, f) (0.634, 100 mm). The red dashed lines depict the external cavity frequency f_{ext} , and the black curves are the spectra without feedback for reference.

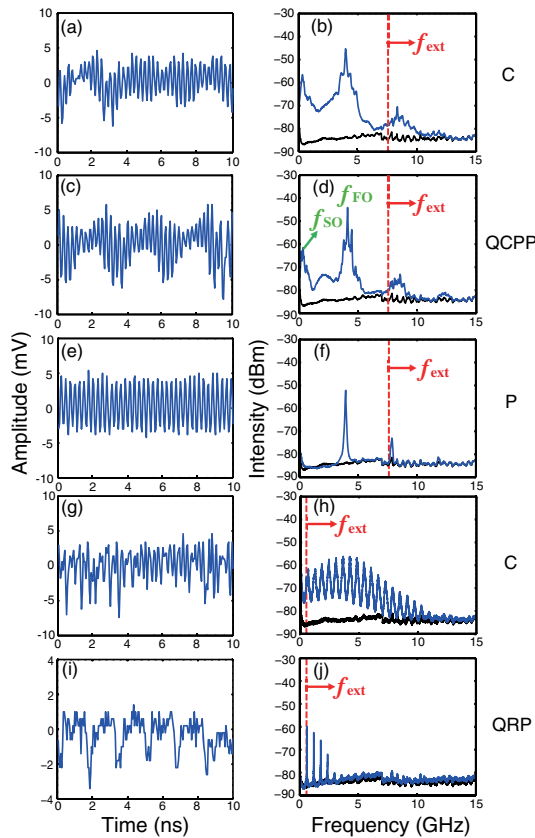


Fig. 4. Time series and corresponding power spectra of the dynamical states obtained experimentally from the ES laser in the SCR and the LCR with $(\xi_f, L_{\text{ext}}) = (a, b) (0.703, 20 \text{ mm})$, $(c, d) (0.686, 20 \text{ mm})$, $(e, f) (0.48, 20 \text{ mm})$, $(g, h) (0.703, 200 \text{ mm})$, and $(i, j) (0.267, 200 \text{ mm})$. The red dashed lines depict the external cavity frequency f_{ext} , and the black curves are the spectra without feedback for reference.

the fast oscillation of this QCPP oscillates at f_{RO} . The f_{SO} is not coincident with either f_{RO} or f_{ext} , but occurs with a frequency of 340 MHz. Moreover, unlike the spectra of typical RPP states that have frequency components of only fast or slow oscillations and their corresponding harmonics and beats, the spectrum of the QCPP state preserves the broadband characteristics as present in the *C* state. When ξ_f further decreases to 0.48, as shown in Figs. 4(e) and 4(f), a *P* state stably oscillating at $f_{\text{FO}} = 4 \text{ GHz}$ is obtained. Increasing L_{ext} to 200 mm into the LCR, a *C* state with a time delay signature corresponding to f_{ext} is obtained at $\xi_f = 0.703$, as shown in Figs. 4(g) and 4(h). When ξ_f decreases to 0.267, a QRP state with periodic drops in intensity, as shown in Figs. 4(i) and 4(j), is found. Unlike typical regular pulsing states that oscillate at a frequency corresponding to f_{RO} , the QRP states oscillate at frequencies coincident with f_{ext} .

Compared to the GS laser which, in general, is stable and insensitive to feedback, the ES laser is more easily moving to complex dynamics. While a GS laser is of large importance for the development of isolator-free transmitters in short-reach networks, an ES laser on the other hand can be essential for applications taking advantages of *C* such as *C* lidars, *C* radars, and high-speed random number generations [29–31].

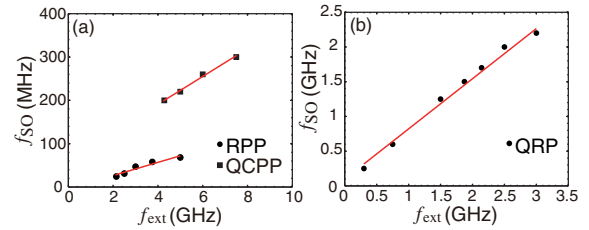


Fig. 5. Slow oscillation frequencies f_{SO} of (a) the RPP and QCPP states and (b) the QRP states under different external cavity frequencies f_{ext} found in the SCR of both GS and ES lasers and the LCR of the ES laser, respectively. The red lines are the linear fits.

Figures 5(a) shows f_{SO} extracted from the RPP states of the GS laser and the QCPP states of the ES laser in their SCRs under different f_{ext} . As can be seen, while f_{SO} does not coincide exactly with either f_{RO} or f_{ext} , f_{SO} in both states it increases linearly as f_{ext} increases. Figure 5(b) shows the f_{SO} extracted from the QRP states under different f_{ext} in the LCR of the ES laser. As can be seen, f_{SO} coincides well with f_{ext} in the QRP states. The slight discrepancy is attributed to the over-estimation in f_{ext} , where the internal laser cavity and the refractive index of optics were neglected when measuring L_{ext} .

Figures 6(a)–6(d) show mappings of the dynamical states of the GS and ES lasers under different feedback conditions at $1.5 \times I_{\text{th}}$ and $1.75 \times I_{\text{th}}$, respectively. The red dashed lines depict the boundaries between the SCR and the LCR. As can be seen in Fig. 6(a), at $1.5 \times I_{\text{th}}$, the GS laser oscillates in FL states when ξ_f exceeds about 0.3 in the LCR. In the SCR, the laser enters *P*, and then RPP states as ξ_f increases. At a larger bias current of $1.75 \times I_{\text{th}}$, as shown in Fig. 6(b), the GS laser becomes even more stable where the region of the steady states (*S*) expanded and ξ_f needed for the laser to excite instability increases. Note that the laser is more sensitive to the feedback phase in the SCR than in the LCR. As can be seen, the edge of the *S* region humps higher in ξ_f (more stable) when the laser is constructively interfered with one of its external cavity modes [28,32].

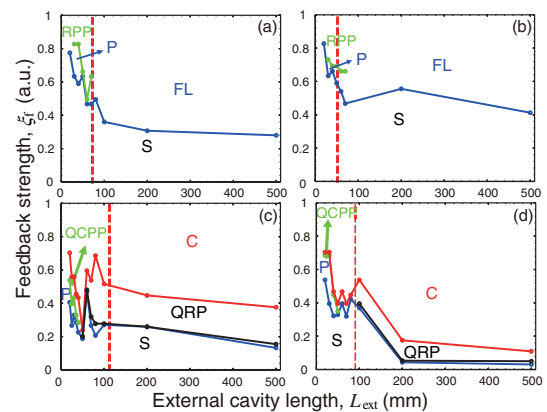


Fig. 6. Mappings of the dynamical states for (a) a GS at $1.5 \times I_{\text{th}}$, (b) a GS at $1.75 \times I_{\text{th}}$, (c) an ES at $1.5 \times I_{\text{th}}$, and (d) an ES at $1.75 \times I_{\text{th}}$ under different feedback conditions, where their corresponding f_{RO} are 2.1, 2.5, 1.3, and 1.7 GHz under free-running conditions, respectively. The red dashed lines depict the respective boundaries of the SCR and the LCR.

For the ES laser at $1.5 \times I_{th}$, as shown in Fig. 6(c), it enters QRP, and then C states as ξ_f increase in the LCR. In the SCR, P and QCPP states are found before the laser enters C states. Note that complex dynamics, especially C states are only found in the ES laser, but not in the GS laser, even for the highest ξ_f attainable in this setup. Moreover, when the bias current increases to $1.75 \times I_{th}$, as shown in Fig. 6(d), the ES laser is easily excitable and can enter C states with a relatively lower ξ_f .

From these results, it is obvious that, although the GS and ES lasers have the same active medium, their response to the feedback is very different. Unlike the ES laser, the carrier dynamics of the GS laser involves transport, capture, and relaxation, leading to a larger damping rate γ_D that stabilizes the laser and prevents the development of complex dynamics. As reported in [25], γ_D of 18 GHz is estimated for this GS laser, while it is only 0.6 GHz for the ES laser. Moreover, the ES laser has a stronger modal competition [25] which also makes it easier to be driven into instabilities.

We investigated the dynamical states and their spectral characteristics of multimode optical feedback QD lasers emitting exclusively on the GS or the ES in both the SCR and LCR. Although these GS and ES lasers are made from the same active medium, their feedback dynamics is found to be very different. The GS laser is shown to be more resistant to feedback, especially at a higher bias level, attributed to its large damping rate. No C states can be found with the attainable feedback parameters in this Letter. P and RPP states are observed in the SCR, and FL states are found in the LCR. Compared to the RPP states reported previously in QW lasers that typically have less than 10 oscillations in a pulse package, the RPP states from the GS laser are densely packed with more than 40 oscillations. Moreover, the fast oscillation frequencies are found to be no longer coincident with f_{ext} , but with f_{RO} .

The ES laser, in contrast, is shown to be easily excitable and can enter C states with a relatively lower ξ_f , especially at a higher bias level. In the SCR, P , QCPP, and then C states emerge as ξ_f increases and, in the LCR, C states are developed after QRP states. While the f_{SO} for RPP and QCPP are much lower than both f_{ext} and f_{RO} , they are shown to be governed and increase linearly with f_{ext} . While the more stable GS laser can be important for the development of isolator-free transmitters benefiting from its great resistance against feedback, the ES laser, on the other hand, is suitable for applications taking advantages of C such as C lidars, C radars, and high-speed random bit generations. Feedback dynamics of InAs/GaAs distributed feedback QD lasers [33] will be investigated in our future work.

Funding. Ministry of Science and Technology, Taiwan (MOST) (103-2112-M-007-019-MY3, 105-2911-I-007-501); Campus France (PhC Orchid No. 33721SC); Institut Mines Télécom (IMT) (the Futurs & Ruptures Program).

REFERENCES

- R. Lang and K. Kobayashi, IEEE J. Quantum Electron. **16**, 347 (1980).
- D. Lenstra, B. Verbeek, and A. Den Boef, IEEE J. Quantum Electron. **21**, 674 (1985).
- T. Heil, I. Fischer, W. Elsässer, and A. Gavrielides, Phys. Rev. Lett. **87**, 243901 (2001).
- M. Sciamanna, A. Tabaka, H. Thienpont, and K. Panajotov, J. Opt. Soc. Am. B **22**, 777 (2005).
- T. Heil, I. Fischer, W. Elsässer, B. Krauskopf, K. Green, and A. Gavrielides, Phys. Rev. E **67**, 066214 (2003).
- A. Gavrielides, T. C. Newell, V. Kovanis, R. G. Harrison, N. Swanston, D. Yu, and W. Lu, Phys. Rev. A **60**, 1577 (1999).
- G. Lythe, T. Erneux, A. Gavrielides, and V. Kovanis, Phys. Rev. A **55**, 4443 (1997).
- T. Newell, D. Bossert, A. Stintz, B. Fuchs, K. Malloy, and L. Lester, IEEE Photon. Technol. Lett. **11**, 1527 (1999).
- A. A. Ukhonov, A. Stintz, P. G. Eliseev, and K. J. Malloy, Appl. Phys. Lett. **84**, 1058 (2004).
- O. B. Shchekin and D. G. Deppe, Appl. Phys. Lett. **80**, 3277 (2002).
- R. L. Sellin, C. Ribbat, M. Grundmann, N. N. Ledentsov, and D. Bimberg, Appl. Phys. Lett. **78**, 1207 (2001).
- A. Capua, L. Rozenfeld, V. Mikhelashvili, G. Eisenstein, M. Kuntz, M. Laemmlin, and D. Bimberg, Opt. Express **15**, 5388 (2007).
- D. Arsenijević, A. Schliwa, H. Schmeckeber, M. Stubenrauch, M. Spiegelberg, D. Bimberg, V. Mikhelashvili, and G. Eisenstein, Appl. Phys. Lett. **104**, 181101 (2014).
- D. Arsenijević and D. Bimberg, Proc. SPIE **9892**, 98920S (2016).
- D. Gready, G. Eisenstein, M. Gioannini, I. Montrosset, D. Arsenijević, H. Schmeckeber, M. Stubenrauch, and D. Bimberg, Appl. Phys. Lett. **102**, 101107 (2013).
- C. Wang, B. Lingnau, K. Lüdge, J. Even, and F. Grillot, IEEE J. Quantum Electron. **50**, 1 (2014).
- M. Ishida, N. Hatori, T. Akiyama, K. Otsubo, Y. Nakata, H. Ebe, M. Sugawara, and Y. Arakawa, Appl. Phys. Lett. **85**, 4145 (2004).
- F. I. Zubov, M. V. Maximov, E. I. Moiseev, A. V. Savelyev, Y. M. Shernyakov, D. A. Livshits, N. V. Kryzhanovskaya, and A. E. Zhukov, Electron. Lett. **51**, 1686 (2015).
- D. O'Brien, S. Hegarty, G. Huyet, J. McInerney, T. Kettler, M. Laemmlin, D. Bimberg, V. Ustinov, A. Zhukov, S. Mikhlin, and A. Kovsh, Electron. Lett. **39**, 1819 (2003).
- D. O'Brien, S. P. Hegarty, G. Huyet, and A. V. Uskov, Opt. Lett. **29**, 1072 (2004).
- E. A. Viktorov, P. Mandel, I. O'Driscoll, O. Carroll, G. Huyet, J. Houlihan, and Y. Tanguy, Opt. Lett. **31**, 2302 (2006).
- M. Virte, S. Breuer, M. Sciamanna, and K. Panajotov, Appl. Phys. Lett. **105**, 121109 (2014).
- F. Grillot, C. Y. Lin, N. A. Naderi, M. Pochet, and L. F. Lester, Appl. Phys. Lett. **94**, 153503 (2009).
- D. Arsenijević, M. Kleinert, and D. Bimberg, IEEE Photon. J. **6**, 700306 (2014).
- H. Huang, D. Arsenijević, K. Schires, T. Sadeev, D. Bimberg, and F. Grillot, AIP Adv. **6**, 125114 (2016).
- A. R. Kovsh, N. A. Maleev, A. E. Zhukov, S. S. Mikhlin, A. P. Vasil'ev, E. A. Semenova, Y. M. Shernyakov, M. V. Maximov, D. A. Livshits, V. M. Ustinov, N. N. Ledentsov, D. Bimberg, and Z. I. Alferov, J. Cryst. Growth **251**, 729 (2003).
- F. Y. Lin and J. M. Liu, Appl. Phys. Lett. **81**, 3128 (2002).
- J. Ohtsubo, *Semiconductor Lasers: Dynamics of Semiconductor Lasers with Optical Feedback*, Springer Series in Optical Sciences (Springer, 2017).
- F. Y. Lin and J. M. Liu, IEEE J. Sel. Top. Quantum Electron. **10**, 991 (2004).
- F. Y. Lin and J. M. Liu, IEEE J. Quantum Electron. **40**, 815 (2004).
- R. Takahashi, Y. Akizawa, A. Uchida, T. Harayama, K. Tsuzuki, S. Sunada, K. Arai, K. Yoshimura, and P. Davis, Opt. Express **22**, 11727 (2014).
- L. C. Lin, S. H. Liu, and F. Y. Lin, Opt. Express **25**, 25523 (2017).
- M. Stubenrauch, G. Stracke, D. Arsenijević, A. Strittmatter, and D. Bimberg, Appl. Phys. Lett. **105**, 011103 (2014).